CERN-ACC-NOTE-2019-0021

13 June 2019
helga.timko@cern.ch

LHC MDs 3163, 3164, and 3166: Injection oscillations throughout the cycle

H. Timko, T. Argyropoulos, P. Baudrenghien, R. Calaga, I. Karpov, L. Medina Medrano, F. Peauger, E. Shaposhnikova, K. Turaj
CERN, CH-1211 Geneva, Switzerland

Keywords: machine development, injection oscillations, controlled emittance blow-up

Summary

This note summarises three inter-related machine development sessions that were performed in the LHC in the course of 2018. Long-lasting injection oscillations and beam stability at injection were investigated as a function of capture voltage in the MD 3164 on optimal injection voltage. The convergence of bunch lengths during the controlled emittance blow-up applied in the acceleration ramp was studied in the MD 3163. Finally, the bunch distribution at arrival to flat top was observed using peak-detected Schottky spectra in the MD 3166.

MD 3163 took place on 27th July 2018 between 03:00 and 11:00
MD 3164 took place between 15th June 2018 23:00 and 16th June 2018 07:00
MD 3166 took place on 15th September 2018 between 16:00 and 19:30

Contents

Data folders

The data acquired during and analysed after the MDs can be found in the following NFS folders:

- MD3163: `/user/slops/data/LHC_DATA/OP_DATA/RFMDs/2018-07-27_BUP`
- MD3164: `/user/slops/data/LHC_DATA/OP_DATA/RFMDs/2018-06-15_optInjVoltage`
- MD3166: `/user/slops/data/LHC_DATA/OP_DATA/RFMDs/2018-09-15_hole`

1 Ramps with different blow-up settings

The controlled emittance blow-up in the ramp has been studied in the MD3163. Various blow-up spectra, target bunch lengths, and initial bunch lengths have been investigated. The data collected in these MDs shall be used to benchmark multi-bunch simulations of the controlled emittance blow-up. The simulations, in turn, will hopefully give insight into the bunch length divergence observed for small target bunch lengths.

1.1 Ramp 1 (fill 6988)

In the first fill, 12 b and 144 b were injected in 4 MV capture voltage. After that, the voltage was increased to 6 MV and another 144 b were injected. Finally, a third batch of 144 b were injected in 8 MV. In the accelerating ramp, the voltage was increased linearly from 8 MV to 12 MV. The average bunch intensity was $(1.01 \pm 0.05) \times 10^{11}$ p/b in both rings.

The target bunch length was 0.9 ns constant, and the blow-up spectrum was adjusted to the corresponding bandwidth of 0.944587...1.05$\times f_{s,0}$. A spectrum with pre-distortion was used to counteract the action of the beam phase loop; the pre-distortion was calculated for a 0.9 ns parabolic bunch distribution, see Fig. 1.

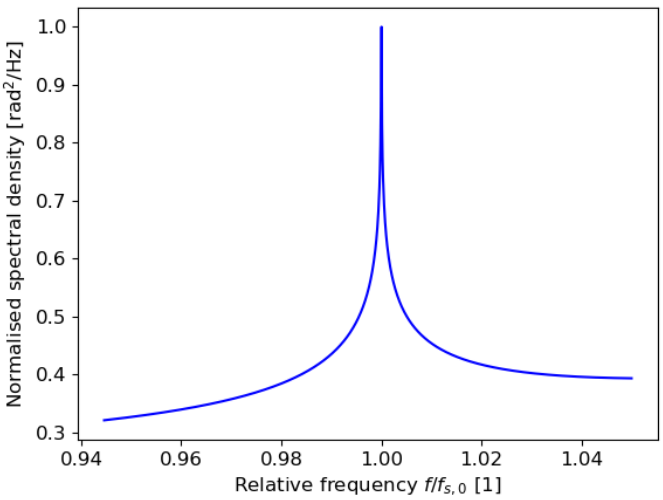

Figure 1: Blow-up spectrum used in Ramps 1 and 2. The frequency range is relative to the central synchrotron frequency, and the spectral density is normalised to 1.

The resulting bunch length evolution is shown in Fig. 2. The blow-up is not acting in the beginning of the ramp, as the bunches are on average longer than the target value. As a measure of beam stability, we compare the bunch length evolution to the threshold of loss of Landau damping, established for single bunches in LHC MDs previously [1]:

$$\xi_{\mathsf{th}} \equiv \frac{\tau^5 V}{N_b} = (5.0 \pm 0.5) \times 10^{-5}\,\mathsf{ns}^5\mathsf{V}\,, \tag{1}$$

where τ is the 4-sigma equivalent FWHM bunch length as measured by the BQM, V is the RF voltage, and N_b is the bunch intensity. The energy dependence is implicitly contained in

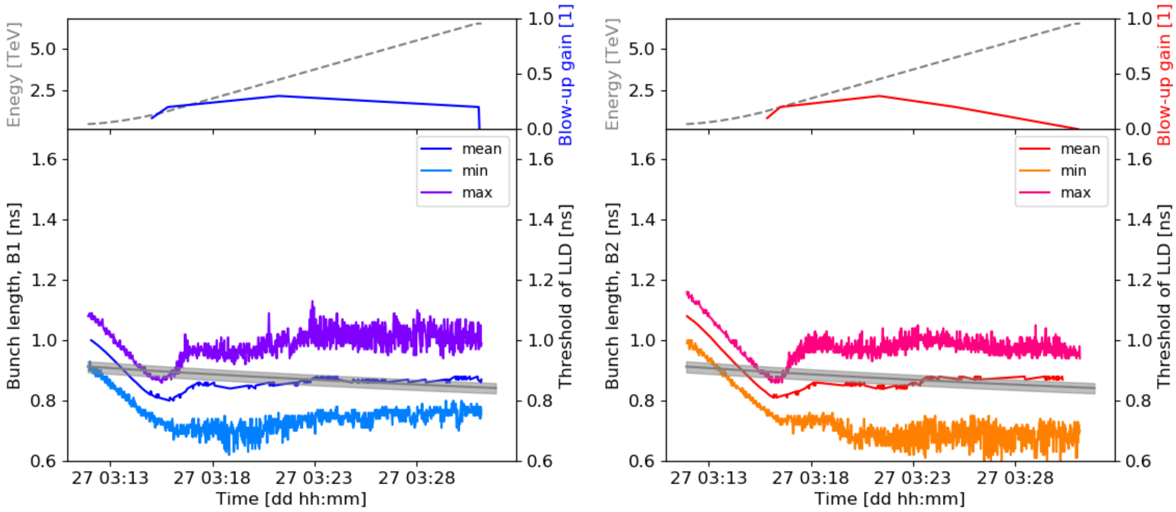

Figure 2: Fill 1: average bunch length evolution during the controlled emittance blow-up; B1 (left) and B2 (right). The bottom plots show the evolution of the average, minimum and maximum bunch length over the ring, compared to the bunch length threshold of loss of Landau damping (gray). The top plots show the blow-up gain (coloured) and the synchronous energy (gray) during the acceleration ramp.

the bunch length and voltage dependence. The plots show the minimum bunch length, with error bar, required for single-bunch stability,

$$\tau_{\mathrm{th}} \equiv \left(\frac{\xi_{\mathrm{th}} N_b}{V}\right)^{1/5}. \tag{2}$$

Figure 2 shows that the average bunch length remains close to the threshold of loss of Landau damping throughout the fill, which was the goal of this test. As expected, the bunches diverge more than operationally, with the minimum-to-maximum bunch length spread[1] being 254 ps (B1) and 263 ps (B2) at arrival to flat top. The shortest bunches barely blow up, while others blow up more than targeted.

There is no significant difference in terms of intensity or bunch length evolution between the three batches of 144 b, which were captured with different voltage, as is shown in Fig. 3. However, it is expected that the batches captured in a larger voltage (and thus with a larger mismatch) have a larger oscillation amplitude, at least initially. This could affect the quality of the blow-up. Indeed, the third batch that has been injected in 8 MV exhibits a larger bunch length spread at arrival to flat top. The phenomenon is to be studied in more details in the future.

[1]The minimum-maximum spread is calculated as the time average of the last 10 points before arrival to flat top.

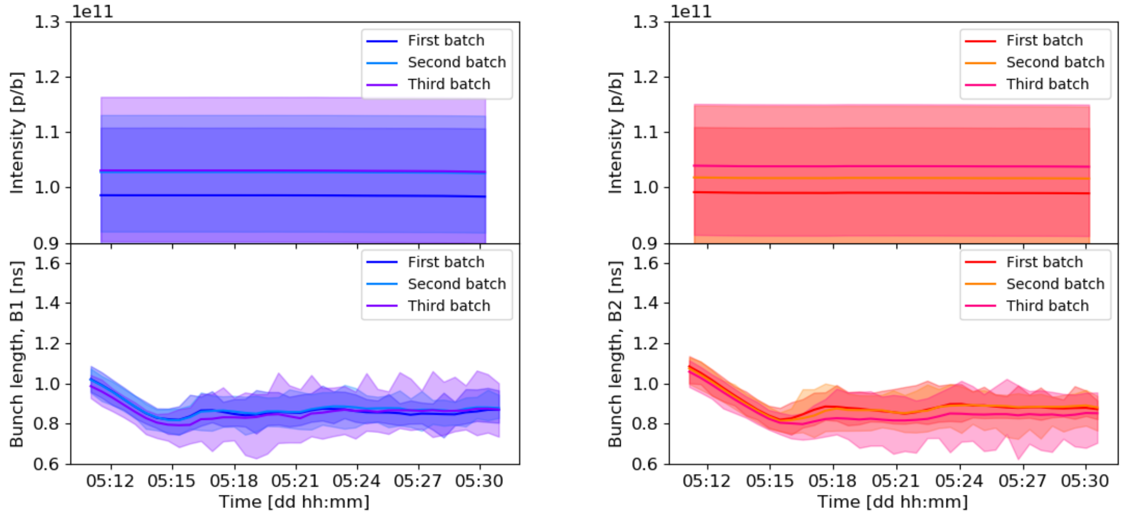

Figure 3: Fill 1: intensity (top) and bunch length evolution (bottom) of the three batches of 144 b during the ramp.

1.2 Ramp 2 (fill 6989)

In this fill, the injection procedure and the voltage programme during the ramp was just like in Ramp 1. The average bunch intensity was $(1.10 \pm 0.06) \times 10^{11}$ p/b in B1 and $(1.07 \pm 0.07) \times 10^{11}$ p/b in B2. The target bunch length was increased to 1.1 ns in the first 800 s of the ramp, for more beam stability. In the last 400 s, the target remained at 0.9 ns. The blow-up spectrum was kept the same as in the previous ramp, i.e. with a frequency band of 0.944587...$1.05 \times f_{s,0}$, and a pre-distortion calculated for a 0.9 ns long parabolic bunch.

Indeed, better beam stability is provided in this case, as seen in Fig. 4. The bunch length spread at arrival to flat top reduces to 193 ps (B1) and 156 ps (B2). B2, blown up already at injection, is better converged at high energy, as the larger initial emittance is providing more stability margin at low energy.

The batch-by-batch behaviour is shown in Fig. 5. The difference in bunch length spread between the different batches is not so prominent this time.

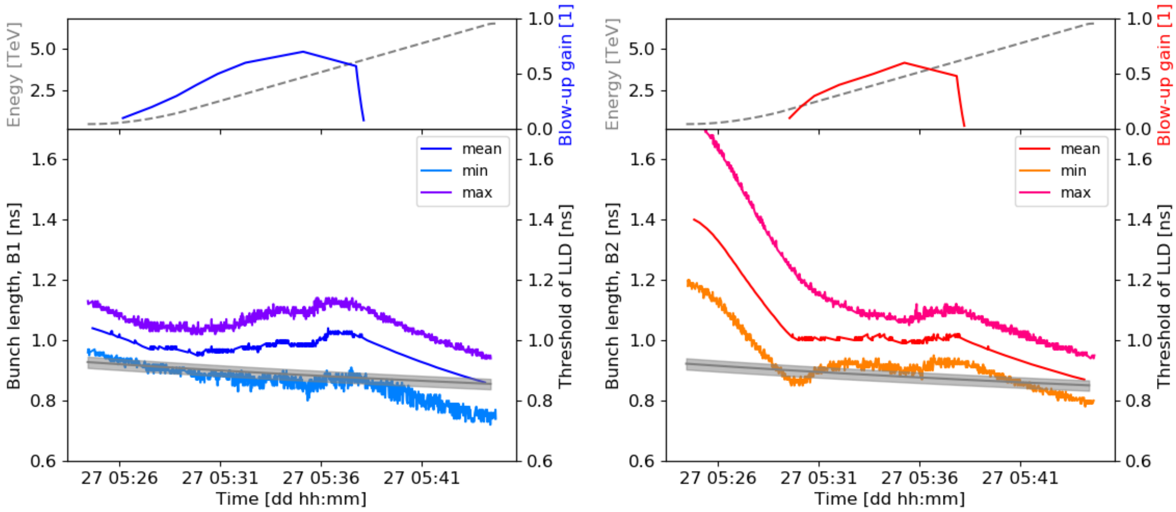

Figure 4: Fill 2: average bunch length evolution during the controlled emittance blow-up; B1 (left) and B2 (right). The bottom plots show the evolution of the average, minimum and maximum bunch length over the ring, compared to the bunch length threshold of loss of Landau damping (gray). The top plots show the blow-up gain (coloured) and the synchronous energy (gray) during the acceleration ramp.

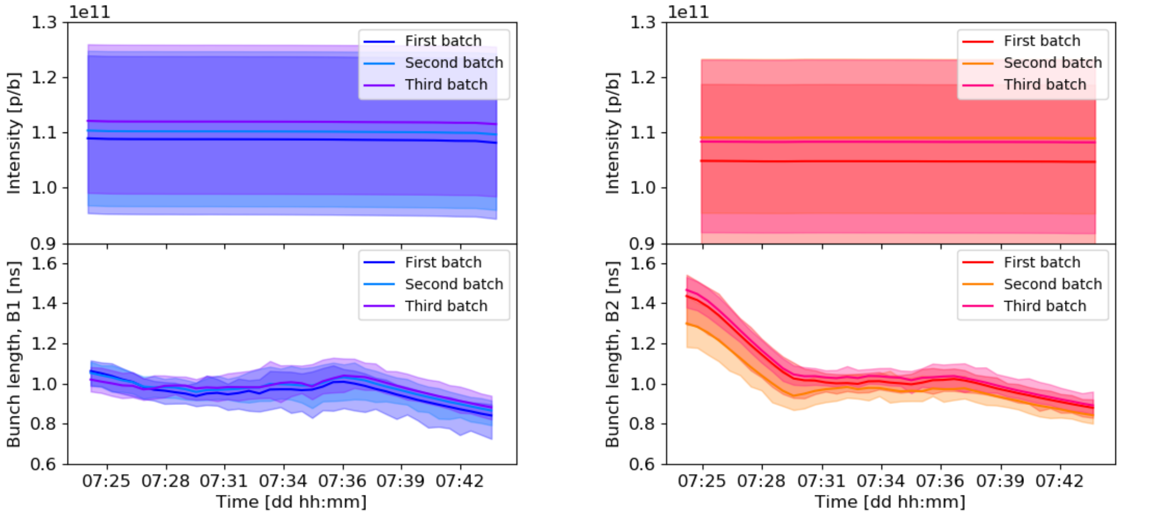

Figure 5: Fill 2: intensity (top) and bunch length evolution (bottom) of the three batches of 144 b during the ramp.

1.3 Ramp 3 (fill 6990)

In the third ramp, the injection voltage was kept constant at 6 MV. First 12 b, and then three batches of 144 b have been injected. The average bunch intensity was $(1.10 \pm 0.04) \times 10^{11}$ p/b in B1 and $(1.10 \pm 0.05) \times 10^{11}$ p/b in B2. For the trains of 144 b, the emittance has been varied in the SPS; the average bunch length at extraction from the SPS was 1.75 ns, 1.65 ns, and 1.48 ns, respectively. The ramp was performed with a linear voltage increase from 6 MV to 12 MV, as in nominal fills.

For the emittance blow-up, the target bunch length was 1.1 ns constant throughout the ramp. The frequency bandwidth of the blow-up spectrum was adapted to $0.917223...1.05 \times f_{s,0}$, with the pre-distortion being calculated for a bunch length of 1.1 ns, see Fig. 6.

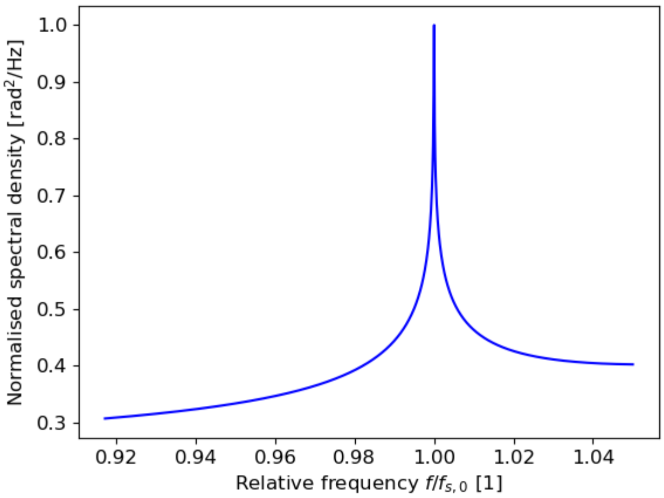

Figure 6: Blow-up spectrum used in Ramp 3. The frequency range is relative to the central synchrotron frequency, and the spectral density is normalised to 1.

Most bunches are above the threshold of loss of Landau damping at all times, see Fig. 7. Despite the large bunch length spread after injection, good convergence is therefore achieved;

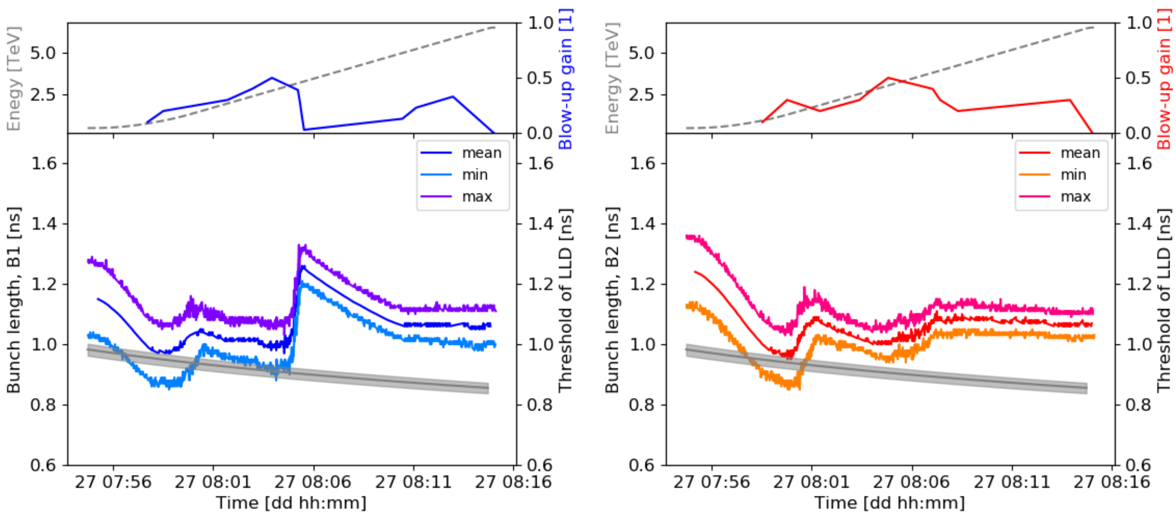

Figure 7: Fill 3: average bunch length evolution during the controlled emittance blow-up; B1 (left) and B2 (right). The bottom plots show the evolution of the average, minimum and maximum bunch length over the ring, compared to the bunch length threshold of loss of Landau damping (gray). The top plots show the blow-up gain (coloured) and the synchronous energy (gray) during the acceleration ramp.

the bunch length spread at arrival to flat top is as small as 118 ps (B1) and 84 ps (B2).

Figure 8 shows the batch-by-batch signature. Despite the difference in initial bunch

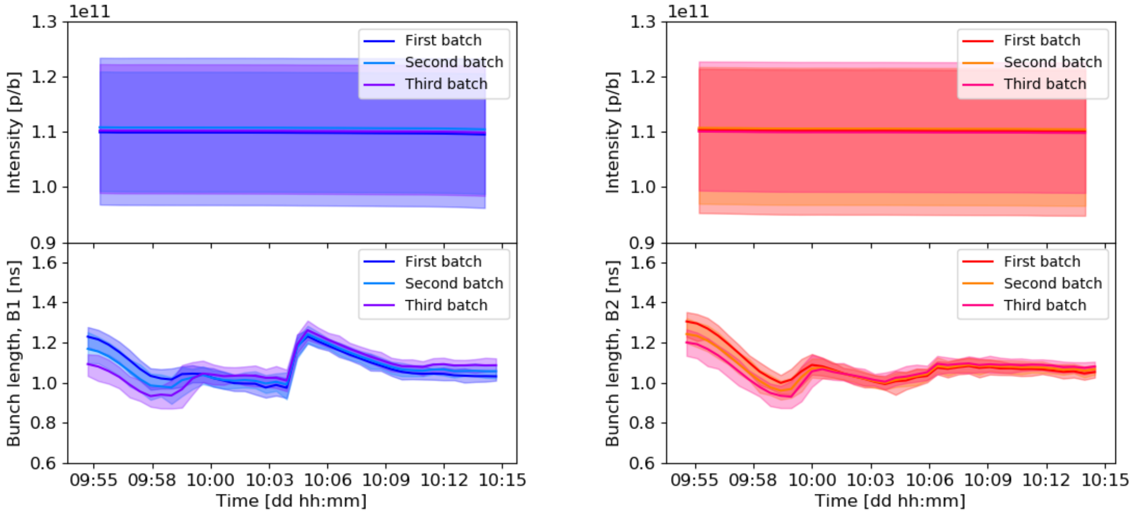

Figure 8: Fill 3: intensity (top) and bunch length evolution (bottom) of the three batches of 144 b during the ramp.

lengths, the blow-up manages to make the bunch lengths converge at arrival to flat top.

1.4 Ramp 4 (fill 6991)

Finally, 20 single bunches were injected in 6 MV for studies of the bunch distribution at arrival to flat top (see Sec. 2). The average bunch intensity was $(1.10 \pm 0.04) \times 10^{11}$ p/b in B1 and $(1.08 \pm 0.03) \times 10^{11}$ p/b in B2. Also in this case, the ramp was performed with a linear voltage increase from 6 MV to 12 M. The operational blow-up settings were used: a target bunch length of 1.25 ns in the first 800 s, then reduced to 1.1 ns in the subsequent 400 s, with a blow-up spectrum covering 0.8571...1.05$\times f_{s,0}$, using a pre-destortion for 1.25 ns, , see Fig. 9.

In this fill, all bunches are well above the threshold bunch length, see Fig. 10. The bunch length spread at arrival to flat top is similar to the operational value seen with batches (typically about 50 ps), in this case 46 ps in B1 and 66 ps in B2.

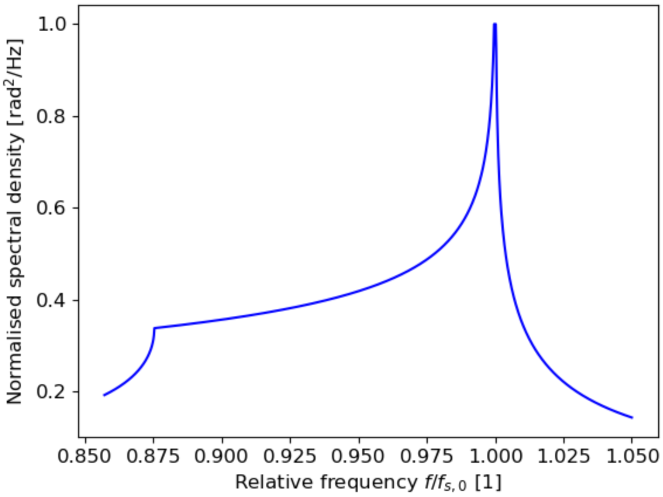

Figure 9: Blow-up spectrum used nominally and in Ramp 4. The frequency range is relative to the central synchrotron frequency, and the spectral density is normalised to 1.

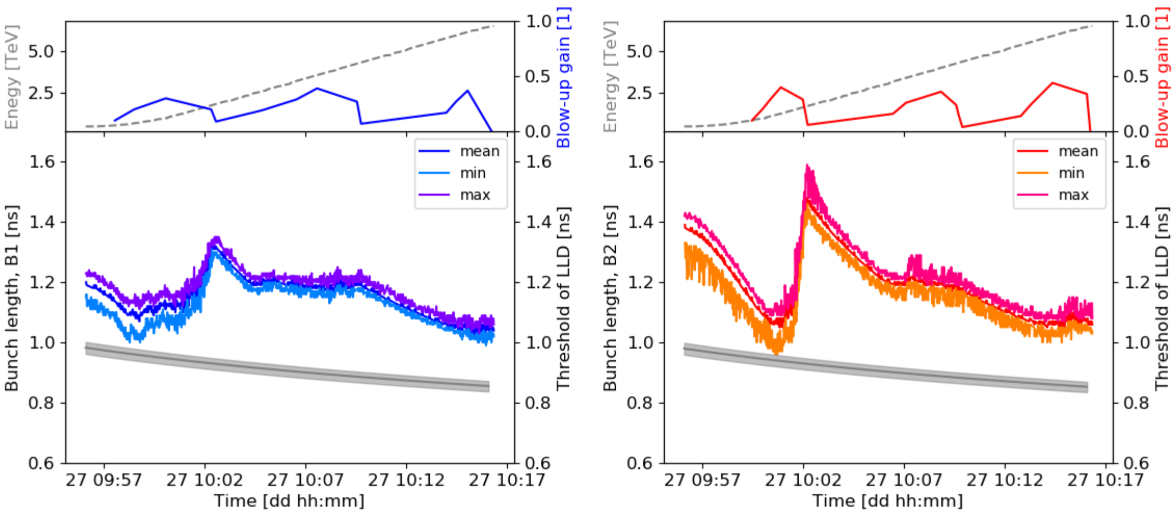

Figure 10: Fill 4: average bunch length evolution during the controlled emittance blow-up; B1 (left) and B2 (right). The bottom plots show the evolution of the average, minimum and maximum bunch length over the ring, compared to the bunch length threshold of loss of Landau damping (gray). The top plots show the blow-up gain (coloured) and the synchronous energy (gray) during the acceleration ramp.

1.5 Summary on blow-up

In conclusion, the more stability margin is kept during the ramp, the smaller the bunch length spread at arrival to flat top.

In all four test, the bunch length at start of the ramp is systematically longer in B2 than in B1. Investigations of SPS-LHC energy mismatch showed previously that B2 has often a worse matching than B1, leading to a larger blow-up after injection.

2 Depleted area in bunch spectrum

In a previous MD with 20 single bunches, a depleted area in the peak-detected Schottky spectrum was observed at arrival to flat top [2]; in that MD, a voltage ramp from 6 MV to 12 MV was used during acceleration. Although this hole was clearly seen on the bunch spectrum, it was not visible on the high-resolution (40 GS/s) bunch profiles. As the mechanism of the depletion was not clear, we performed several tests in this MD to investigate different possible sources.

2.1 Test 1 (fill 7182)

This test took place during MD3166. In this fill, we injected 20 batches of 48 bunches using the filling scheme `Multi_20inj_48bpi_MD3166_RFMD3_2018`. During acceleration, the RF voltage was ramped linearly from 6 MV to 12 MV as in [2]. The aim was to verify that w.r.t. the hole in the bunch distribution, single bunches and batched beam behave in the same way. The hole in the distribution can have an impact on the stability of the bunches, and thus it is important to verify whether it is present also for the operational batched beam.

The ramp took place from 18:11:35 to 18:31:59. All bunches whose peak-detected Schottky spectrum was measured exhibited, to a larger or smaller degree, the depleted area close to the bunch core at arrival to flat top; two examples are shown in Fig. 11.

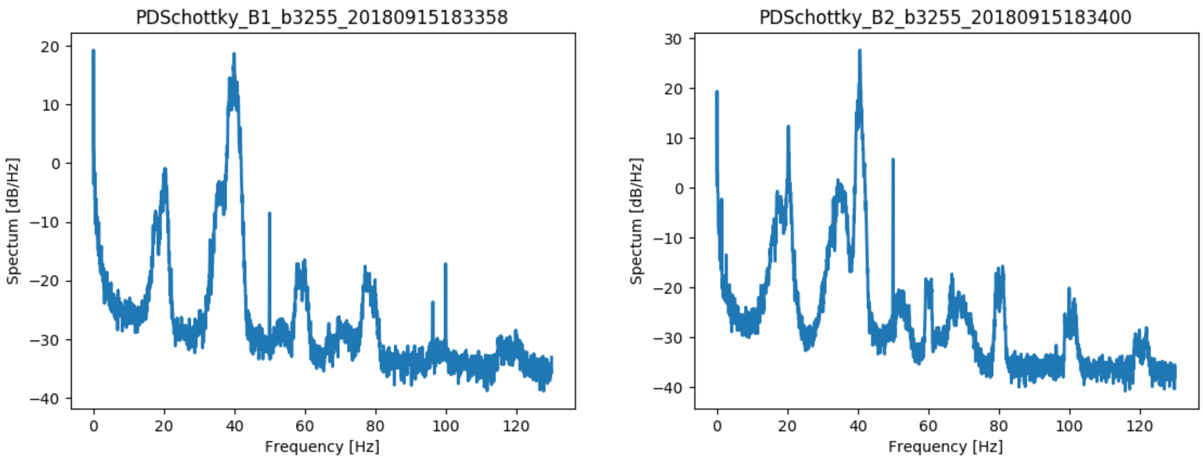

(a) B1, bucket 32551, 18h34

(b) B2, bucket 32551, 18h34

Figure 11: Test 1: peak-detected Schottky spectra shortly after arrival to flat top and opening of the beam phase loop. A depleted area is seen around ~ 38 Hz, somewhat below the quadrupolar central synchrotron frequency of 2×20.64 Hz.

Briefly after arrival to flat top, the beam phase loop was opened on both beams. The hole was replenished due to the natural RF noise of the RF system typically within about 10 minutes, see Fig. 12. In general, B1 has a less prominent hole in the spectrum, which is consequently replenished faster after opening the beam phase loop.

Looking at the peak-detected Schottky spectrum during the acceleration ramp, the hole becomes typically more prominent towards the end of the ramp, at high energies. This can be seen for instance from the waterfall plot in Fig. 13.

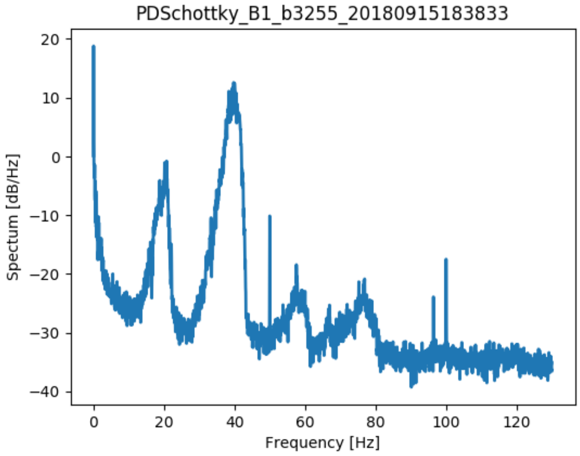

(a) B1, bucket 32551, 18h38

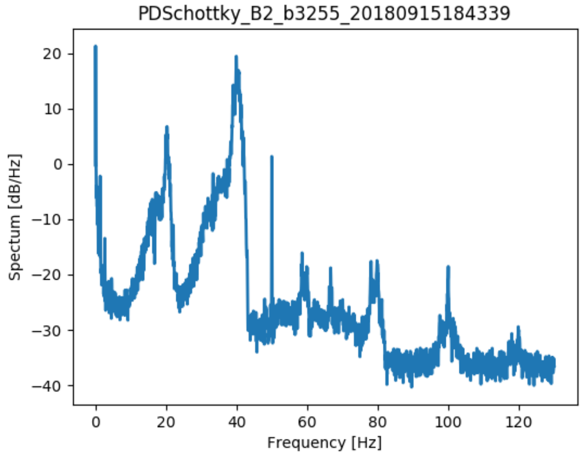

(b) B2, bucket 32551, 18h43

Figure 12: Test 1: peak-detected Schottky spectra 5-10 minutes after opening the beam phase loop. A depleted area is almost replenished on both beams.

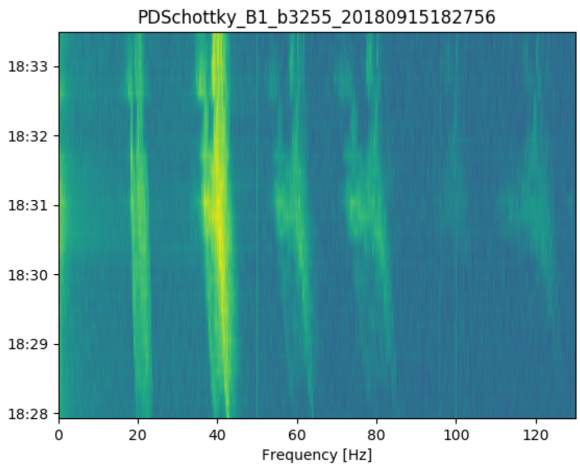

(a) B1, bucket 32551

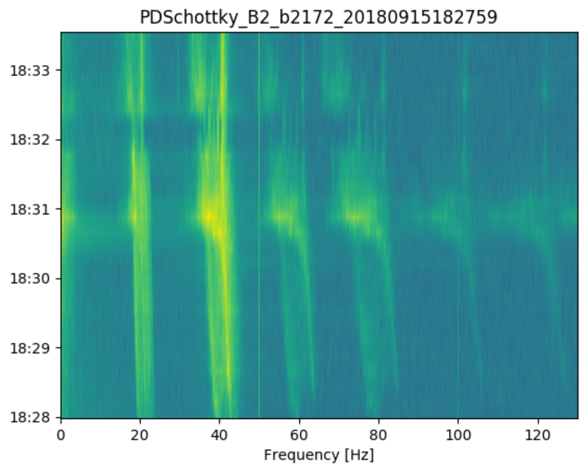

(b) B2, bucket 21721

Figure 13: Test 1: peak-detected Schottky spectra as a function of time (y-axis). The ramp finishes at 18:31:59. The bunches are excited by the controlled emittance blow-up just before arrival to flat top.

2.2 Test 2 (fill 7183)

This test took place during MD3166 as well. In this fill, we injected 20 single bunches using the filling scheme `Single_20b_RFMD3_2018`. During acceleration, the RF voltage was ramped linearly from 4 MV to 12 MV. The central synchrotron frequency thus does not cross the 50 Hz line, as opposed to the ramps that start from 6 MV. At 50 Hz, the background RF noise is more elevated than at other frequencies, due to noise from the electrical grid. The test took place in order to verify whether the hole forms due to the 50 Hz crossing or not.

The ramp took place from 20:19:30 to 20:39:50 and the beam phase loop was opened right after arriving to flat top. The hole is still seen at arrival to flat top, for all bunches examined; an example is shown in Fig. 14. Note that this time, there is no striking difference

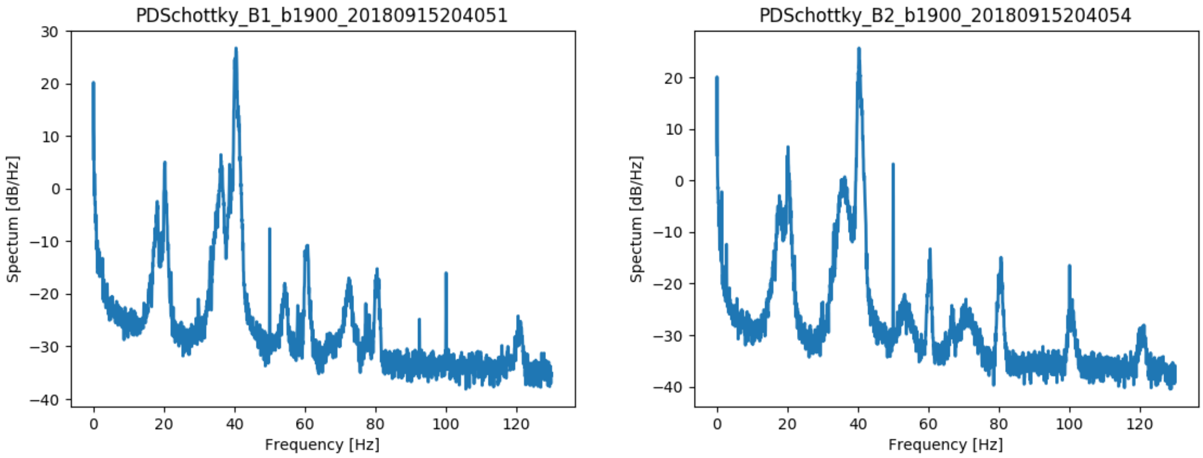

(a) B1, bucket 19001, 20h41

(b) B2, bucket 19001, 20h41

Figure 14: Test 2: peak-detected Schottky spectra shortly after arrival to flat top and opening of the beam phase loop.

observed between B1 and B2.

Again, the hole is replenished within about 10 minutes after opening the beam phase loop, see Fig. 15.

The evolution of the spectra during the ramp is shown in Fig. 16.

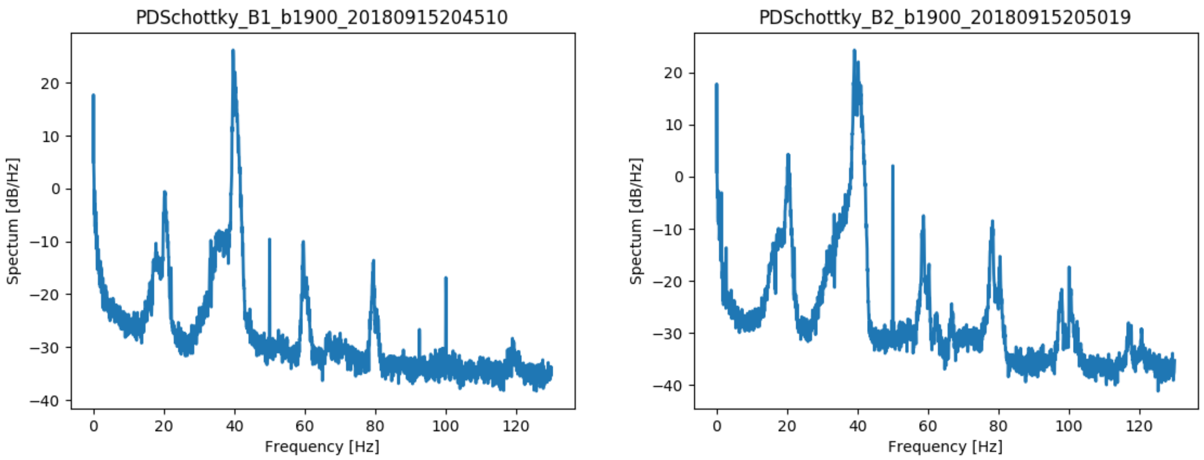

(a) B1, bucket 19001, 20h45

(b) B2, bucket 19001, 20h50

Figure 15: Test 2: peak-detected Schottky spectra 5-10 minutes after opening the beam phase loop. A depleted area is almost replenished on both beams.

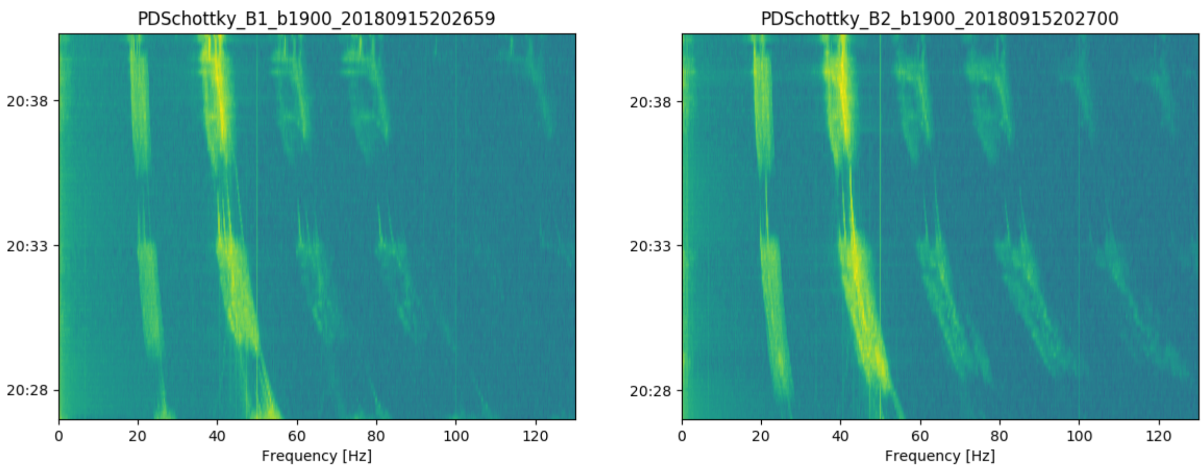

(a) B1, bucket 19001

(b) B2, bucket 19001

Figure 16: Test 2: peak-detected Schottky spectra as a function of time (y-axis). The ramp finishes at 20:39:50.

2.3 Test 3 (fill 6991)

In the last fill of MD3163 discussed in the previous Section, we also took peak-detected Schottky spectra of the 20 nominal single bunches accelerated with a voltage ramp from 6 MV to 12 MV; these were the same conditions as in 2016 [2].

The ramp took place from 11:56:07 to 12:16:21 and the beam phase loop was opened right after arriving to flat top. The test confirms the results of 2016 can be reproduced, see Figs. 17 and 18. [h]

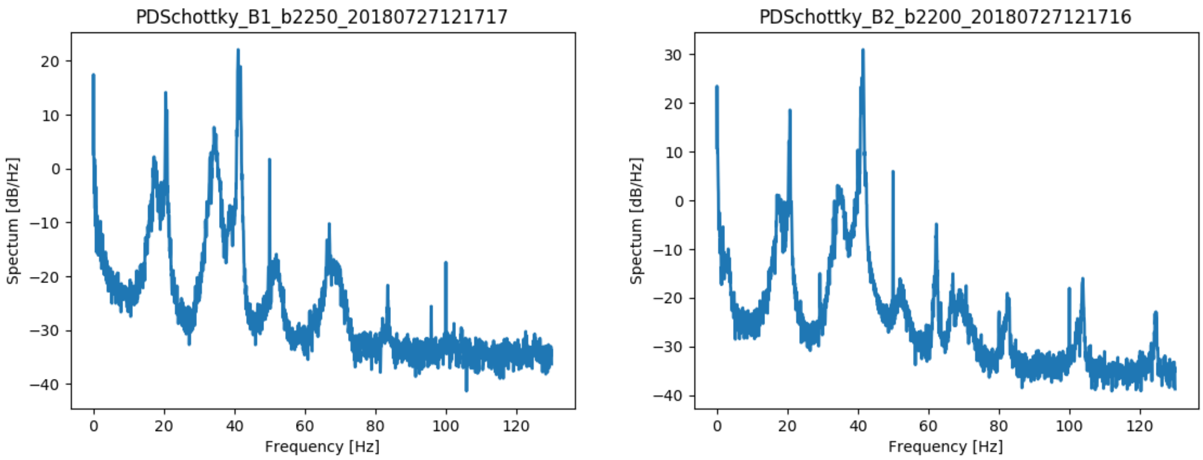

(a) B1, bucket 22501, 12h17

(b) B2, bucket 22001, 12h17

Figure 17: Test 3: peak-detected Schottky spectra shortly after arrival to flat top and opening of the beam phase loop.

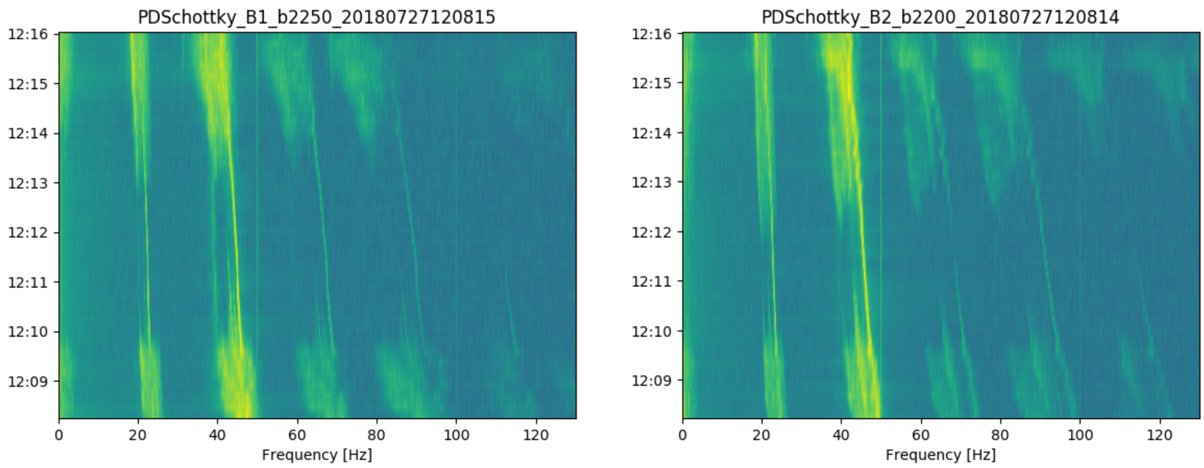

(a) B1, bucket 22501

(b) B2, bucket 22001

Figure 18: Test 3: peak-detected Schottky spectra as a function of time (y-axis). The ramp finishes at 12:16:21.

2.4 Test 4 (fill 6809)

This test was performed during MD3164, with batches of 96 b and 144 b in the nominal injection scheme `25ns_2556b_2544_2215_2332_144bpi_20injV3`; not all batches were injected though. The voltage was ramped from 4 MV to 12 MV; this was a verification that with batched beam and no 50 Hz line crossing the depleted area is still seen. This type of measurement was never done with the operational beam before, as it requires opening the beam phase loop for a few minutes after arrival to flat top.

The ramp took place from 06:12:22 to 06:33:05 and the beam phase loop was opened about two minutes after arriving to flat top. Out of the four bunches measured, none of the bunches in B1 exhibited the hole, while it was present on three out of four bunches in B2; two examples are shown in Fig. 19. The 50 Hz line is more prominent on these spectra. As

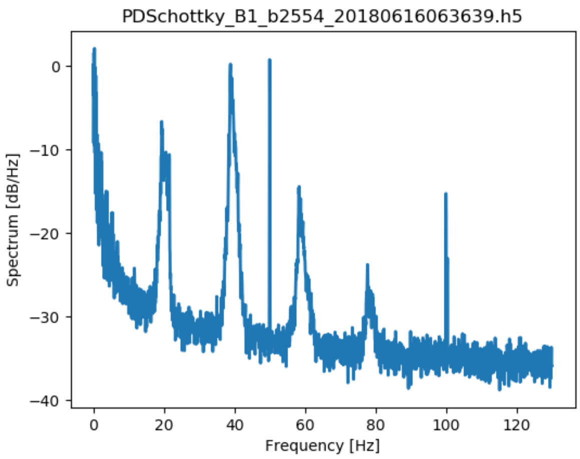

(a) B1, bucket 25541, 12h17

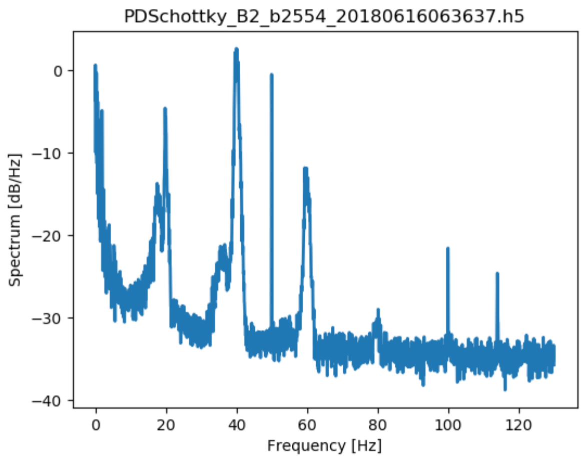

(b) B2, bucket 25541, 12h17

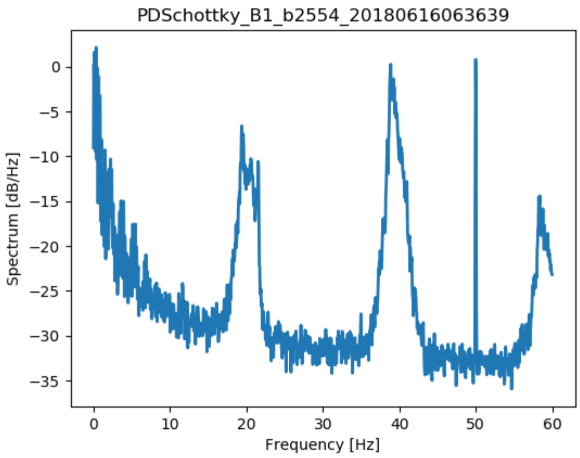

(c) B1, bucket 25541, 12h17, zoom

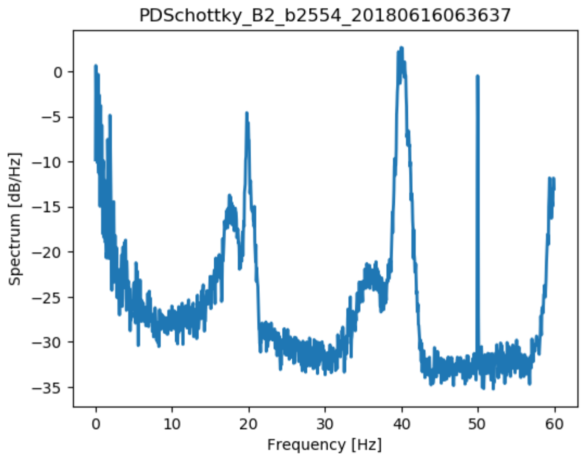

(d) B2, bucket 25541, 12h17, zoom

Figure 19: Test 4: peak-detected Schottky spectra shortly after arrival to flat top and opening of the beam phase loop.

before, the hole fills up within a few minutes with beam phase loop open. Concerning the difference between B1 and B2, the correlation with the controlled emittance blow-up should be investigated in the future. During the operational blow-up scheme, the blow-up is mainly acting in the first 800 s of the ramp, after which the bunches are shrinking adiabatically. Occasionally, the blow-up activates again towards the end of the ramp; this could potentially influence the bunch distribution at arrival to flat top.

2.5 Summary of tests

In summary, the 2018 tests together with the MD in 2016 [2] confirm that

- the hole in the distribution forms both for single bunches and batched beam, when the central synchrotron frequency crosses the 50 Hz line during the ramp (Test 1);
- the hole also forms with single bunches and batches when the 50 Hz line is not crossed (Tests 2 and 4);
- 2016 results with single bunches and 50 Hz line crossing could be reproduced (Test 3).

We can thus conclude that the depleted area forms during the ramp, for single and multi-bunch beam, independent of the 50 Hz line crossing. A potential source for the depleted area in the bunch distribution is the controlled emittance blow-up applied during the ramp; this remains subject of future studies.

3 Optimum injection voltage

In this MD, we varied the capture voltage in the LHC, thus scanning different mismatch values between the energy spread of the arriving bunch and the bucket height of the capturing bucket. We injected nominal intensity batches with the nominal filling scheme, `25ns_2556b_2544_2215_2332_144bpi_20injV3`. For every re-fill of the machine, we injected in total six batches in the following order: one batch of 12 b, two batches of 144 b, and finally three batches of 96 b. The aim was to study the bunch oscillations for different voltages. As the beam phase loop is acting during the filling and averaging over all circulating bunches in the machine, we injected first the longer batches, such that the shorter batches injected later would see a negligible phase correction from the beam phase loop.

Non-rigid dipole oscillations have been observed previously [3], as a consequence of a combination of different effects [4]: (i) mismatch at injection, (ii) injection errors in energy and/or phase, and (iii) intensity effects. To have a reasonable phase error at injection, we first adjusted the injection error with 6 MV injection voltage and one batch of 144 b. After that, we intentionally trimmed the injection phase to have a $10°$ phase error.

The bunch profiles of the last batch of 96 b have been analysed in detail, and their bunch length oscillation amplitude has been extracted as a function of time; a comparison with different voltages is shown in Fig. 20. The damping time and the synchrotron frequency in Fig. 20 have been extracted from the evolution of the bunch length oscillations by a damped sine-wave fit, see Fig. 21.

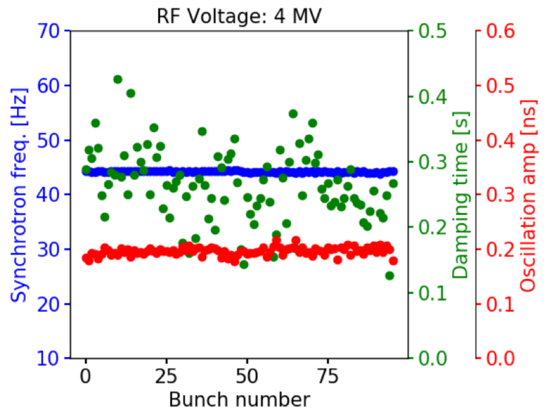

(a) B1, 4 MV, last 96 b

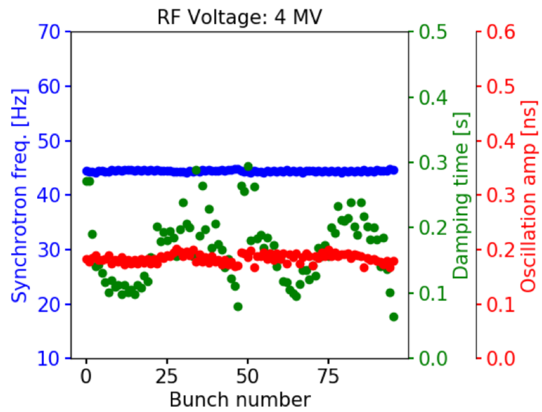

(b) B2, 4 MV, last 96 b

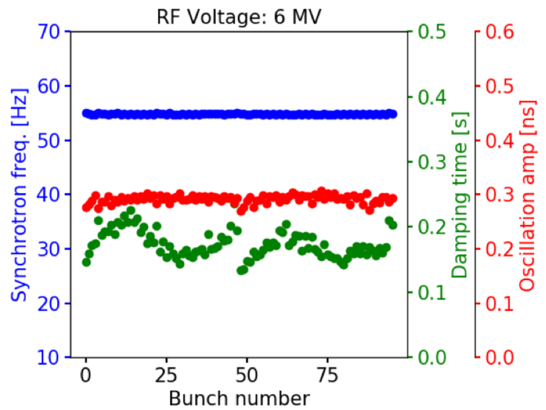

(c) B1, 6 MV, last 96 b

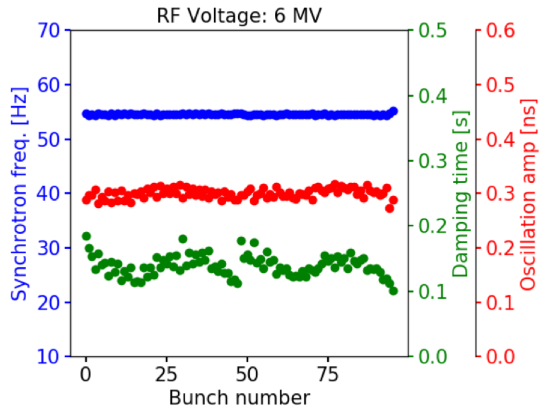

(d) B2, 6 MV, last 96 b

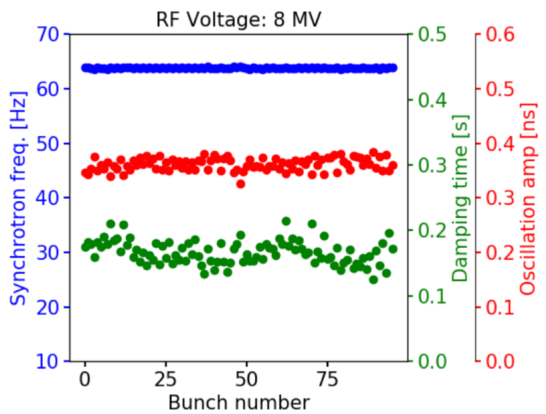

(e) B1, 8 MV, last 96 b

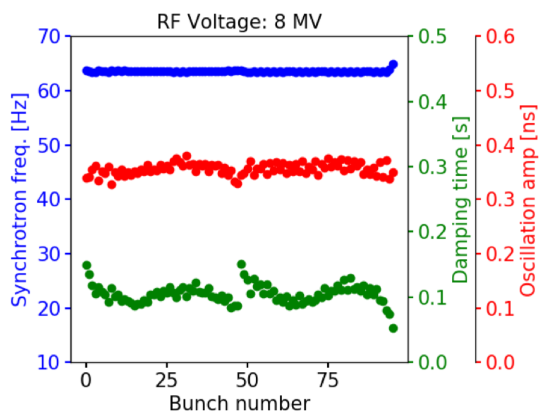

(f) B2, 8 MV, last 96 b

Figure 20: Oscillation amplitude (red), damping time (green), and synchrotron frequency (blue) have been extracted from the bunch profiles of the last 96 b injected. B1 (left) vs. B2 (right), captured in 4 MV (top), 6 MV (middle), and 8 MV (bottom).

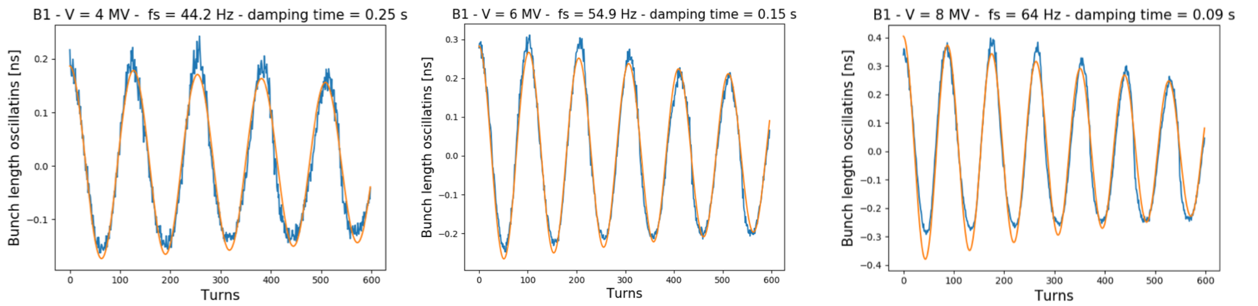

(a) B1, 4 MV (b) B1, 6 MV (c) B1, 8 MV

Figure 21: Extraction of damping time and synchrotron frequency from the bunch length oscillations as a function of time via damped sine-wave fit.

Going from 8 MV through 6 MV to 4 MV, the oscillation amplitude is reduced from about 0.4 ns through 0.3 ns to 0.2 ns, clearly confirming the better matching with lower voltage. The damping time slightly increases with decreased voltage, with significantly more sprea in the measurement at 4 MV. The filamented bunch lengths after injection for different voltages is compared in Fig. 22.

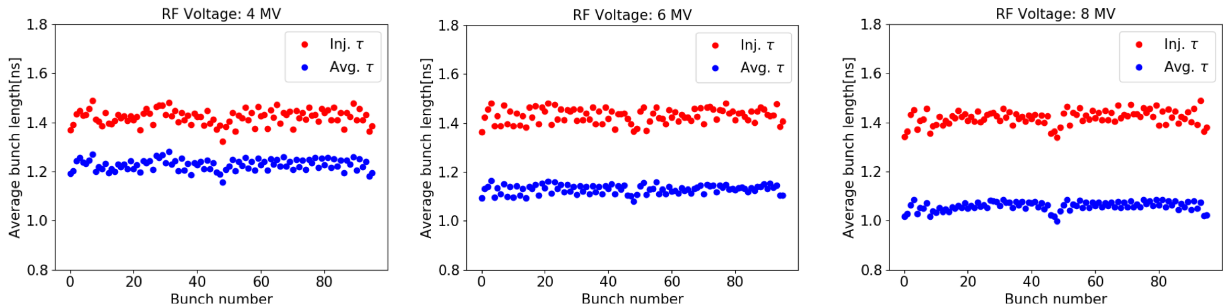

(a) 4 MV (b) 6 MV (c) 8 MV

Figure 22: Injected (red) and filamented (blue) bunch lengths for the last batch of 96 b.

4 Summary

This note summarises the LHC MDs 3163, 3164, and 3166. The MDs were investigating the controlled emittance blow-up during the ramp, the bunch distribution at arrival to flat top, and the optimum injection voltage. For the controlled emittance blow-up, various tests with different noise spectra and target bunch lengths have been made; the data is to be used for benchmarking simulations. Simulation studies, in turn, are planned to investigate the divergence of bunch lengths observed for short target bunch lengths. The MD data indicates that good convergence requires keeping a sufficient stability margin during the ramp w.r.t. the single-bunch threshold of loss of Landau damping.

The controlled emittance blow-up is also a potential cause of the depleted area in the bunch distribution observed close to the core at arrival to flat top. The different measurement tests confirmed that the hole is present both for single bunches and batched beam, whether or not the synchrotron frequency crosses the 50 Hz line or not. This depleted area could affect beam stability at arrival to flat top, and is only observed on the peak-detected Schottky spectra, while it cannot be seen on high-resolution bunch profiles.

Long-lasting injection oscillations have been studied for capture voltages of 4 MV, 6 MV, and 8 MV, in the presence of an injection phase error of 10°. As expected, the oscillation amplitude reduces visibly with the lower, closer-to-matched voltage of 4 MV, while it gets amplified with 8 MV. After the MD, the capture voltage of 4 MV has been used operationally for the rest of the 2018 proton run.

5 Acknowledgements

We thank the LHC operators and energineers in charge for helping us prepare and execute our measurements. We are also very grateful to our RF colleagues, S. Albright, T. Bohl, A. Lasheen, and G. Papotti helping us in the LHC injectors to prepare the beam.

References

[1] J. F. Esteban Müller. *Longitudinal intensity effects in the CERN Large Hadron Collider*. PhD thesis, EPFL, Lausanne, 2016.

[2] Esteban Müller, J. F. and Timko, H. and Baudrenghien, P. and Shaposhnikova, E. LHC MD 232: longitudinal impedance evaluation. Technical report, CERN, Geneva, Switzerland, Mar 2017. CERN-ACC-NOTE-2017-0016.

[3] I. Karpov, S. Albright, T. Argyropoulos, P. Baudrenghien, E. Shaposhnikova, and H. Timko. LHC MD 2042: persistent injection oscillations. Technical report, CERN, Geneva, Switzerland, Feb 2018. CERN-ACC-NOTE-2018-0018.

[4] H. Timko, T. Argyropoulos, I. Karpov, and E. Shaposhnikova. Beam instabilities after injection to the LHC. In *Proc. HB2018 workshop*, Daejeon, Korea, 2018. TUP1WA03.